Coulomb-nuclear interference in pion-nucleus bremsstrahlung

Göran Fäldt* and Ulla Tengblad†

Department of physics and astronomy,

Uppsala University, Box 535, S-751 21 Uppsala,Sweden

Abstract

Pion-nucleus bremsstrahlung offers a possibility of measuring the structure functions of pion-Compton scattering from a study of the small-momentum-transfer region where the bremsstrahlung reaction is dominated by the single-photon-exchange mechanism. The corresponding cross-section distribution is characterized by a sharp peak at small momentum transfers. But there is also a hadronic contribution which is smooth and constitutes an undesired background. In this communication the modification of the single-photon exchange amplitude by multiple-Coulomb scattering is investigated as well as the Coulomb-nuclear interference term.

PACS numbers: 13.60.Fz, 24.10.Ht, 25.80.Hp

*Electronic address: goran.faldt@fysast.uu.se

†Electronic address: ulla.tengblad@fysast.uu.se

I. INTRODUCTION

We shall in this paper add a final touch to the subject of hard bremsstrahlung in pion-nucleus scattering in the Coulomb region. The reaction studied is

$$\pi^- + A \to \pi^- + \gamma + A.$$

In the kinematic region of small momentum transfers to the nucleus the reaction is dominated by the one-photon-exchange mechanism. We have previously derived expressions [1, 2] both for the *Coulomb contribution*, i.e. radiation in conjunction with elastic pion-nucleus-Coulomb scattering , and for the *nuclear contribution*, i.e. radiation in conjunction with elastic pion-nucleus hadronic scattering. Also, detailed predictions for the COMPASS experiment [3] at CERN have been made [4], based on the Coulomb contribution alone. The aim of the COMPASS experiment is to investigate the electromagnetic structure functions of pion-Compton scattering. We studied the senstivity of pionic bremsstrahlung to details of the structure functions by employing a meson-exchange model for the pion-Compton amplitudes that in additon to the Born contributions contained contributions from the σ, ρ, and a_1, exchanges.

Aspects of the theory that need further investigation concern the nuclear background contribution, and the interference between Coulomb and nuclear contributions. These aspects are investigated in the present paper. Also the form factor of the Coulomb amplitude, due to multiple Coulomb scattering, is investigated.

This work extends previous theoretical studies by Gal'perin et al.[5] and Fäldt and Tengblad [1, 2, 4]. The results concerning the Coulomb-form factor may be important for the interpretation of the data by Antipov et al.[6].

The kinematics of the pion-nucleus bremsstrahlung reaction is defined through

$$\pi^-(p_1) + \mathrm{A}(p) \to \pi^-(p_2) + \gamma(q_2) + A(p'), \tag{1}$$

and the kinematics of the related pion-Compton reaction through

$$\pi^-(p_1) + \gamma(q_1) \to \pi^-(p_2) + \gamma(q_2), \tag{2}$$

with $q_1 = p - p'$.

Our analysis is carried for high energies and small transverse momenta, meaning small compared with the longitudinal momenta. In addition the momentum transfer to the nucleus must be in the Coulomb region, i.e. extremely small.

The cross-section distribution is written as

$$\frac{\mathrm{d}\sigma}{\mathrm{d}^2 q_{1\perp}\mathrm{d}^2 q_{2\perp}\mathrm{d}x} = \frac{1}{32(2\pi)^5 E_2\omega_2 M_A^2}\left|\mathcal{M}_{\mathcal{C}} + \mathcal{M}_{\mathcal{N}}\right|^2, \tag{3}$$

where $\mathcal{M}_{\mathcal{C}}$ is the Coulomb amplitude and $\mathcal{M}_{\mathcal{N}}$ the nuclear amplitude. The parameter x is defined as the ratio

$$x = \frac{q_{2z}}{p_1} = \frac{\omega_2}{E_1}, \tag{4}$$

so that e.g., $E_2\omega_2 = x(1-x)E_1^2$. In hadronic bremsstrahlung there is a fixed longitudinal-momentum transfer to the nucleus which depends on x,

$$q_{1\parallel} = q_{min} = \frac{m_\pi^2}{2E_1}\cdot\frac{x}{1-x}. \tag{5}$$

At high energies q_{min} is obviously exceedingly small.

The structure of the cross-section distribution is mainly determined by the one-photon-exchange factor

$$\frac{\boldsymbol{q}_{1\perp}^2}{(\boldsymbol{q}_{1\perp}^2 + q_{min}^2)^2} \tag{6}$$

which vanishes when the transverse-momentum transfer $\boldsymbol{q}_{1\perp}$ to the nucleus vanishes. When the momentum transfer to the nucleus, $q_{1\perp}$, increases far beyond q_{min} we eventually come to momemtum transfers where the nuclear contribution dominates [1].

II. THE COULOMB AMPLITUDE

The expression for the Coulomb amplitude in the one-photon-exchange approximation is given in Eq. (23) of ref.[2]. It reads

$$\mathcal{M}_C^{(B)} \;=\; \frac{8\pi i Z M_A e\alpha}{\mathbf{q}_1^2}\frac{4xE_2}{\mathbf{q}_{2\perp}^2+x^2m_\pi^2}\Big[A(x,\mathbf{q}_{2\perp}^2)\Big(\mathbf{q}_{1\perp}-2\mathbf{q}_{2\perp}\frac{\mathbf{q}_{2\perp}\cdot\mathbf{q}_{1\perp}}{\mathbf{q}_{2\perp}^2+x^2m_\pi^2}\Big)$$

$$+B(x,\mathbf{q}_{2\perp}^2)\mathbf{q}_{1\perp}\Big]\cdot\boldsymbol{\epsilon}_2. \tag{7}$$

The functions $A(x,\mathbf{q}_{2\perp}^2)$ and $B(x,\mathbf{q}_{2\perp}^2)$, which were there called $\tilde{A}(x,\mathbf{q}_{2\perp}^2)$ and $\tilde{B}(x,\mathbf{q}_{2\perp}^2)$, are the pion-Compton-structure functions. Their analytic expressions in the one-meson-exchange approximation are given in the same reference. In the Born approximation, i.e. for point-like pions, the structure functions take the values $A=1$ and $B=0$.

As can be inferred from Eq. (7) the Coulomb amplitude can be factorized as

$$\mathcal{M}_C^{(B)} = \frac{2Z\alpha}{\boldsymbol{q}_{1\perp}^2+q_\parallel^2}\;\boldsymbol{g}\cdot\boldsymbol{q}_1, \tag{8}$$

with the vector $\boldsymbol{g}$ in the impact parameter plane, so that $\boldsymbol{g}\cdot\boldsymbol{q}_1=\boldsymbol{g}\cdot\boldsymbol{q}_{1\perp}$. This amplitude is valid for a point-like nuclear-charge distribution. The factor multiplying $\boldsymbol{g}\cdot\boldsymbol{q}_1$ in Eq.(8) is the π^--nucleus-Coulomb-scattering amplitude in the Born approximation.

The above expression can be improved by taking into account the finite extension of the nuclear-charge distribution and the distortion of the pion trajectory due to Coulomb-multiple scattering. The hadronic distortion is treated in the following section.

In order to simplify notation we drop the index on $\boldsymbol{q}_1$ and put $\boldsymbol{q}_1=\boldsymbol{q}=(\boldsymbol{q}_\perp,q_\parallel)$. Then, observe that expression (8) can be written as

$$\mathcal{M}_C^{(B)}(\boldsymbol{q}) = \frac{2Z\alpha}{\boldsymbol{q}_\perp^2+q_\parallel^2}\;\boldsymbol{g}\cdot\boldsymbol{q} = \frac{-1}{2\pi i}\int \mathrm{d}^3r e^{-i\mathbf{q}\cdot\mathbf{r}}\boldsymbol{g}\cdot\boldsymbol{\nabla}V_C(r), \tag{9}$$

where $V_C(\boldsymbol{r})$ is the Coulomb-point-nucleus potential

$$V_C(\boldsymbol{r}) = -\frac{Z\alpha}{r}, \tag{10}$$

and where $\boldsymbol{g}\cdot\boldsymbol{r}=\boldsymbol{g}\cdot\boldsymbol{b}$ with $\boldsymbol{r}_\perp=\boldsymbol{b}$.

The Coulomb distortion along the pion tractory is in the Glauber model taken into consideration by replacing Eq.(9) by

$$\mathcal{M}_C(\boldsymbol{q}) = \frac{-1}{2\pi i}\int \mathrm{d}^3r e^{-i\mathbf{q}\cdot\mathbf{r}}\boldsymbol{g}\cdot\boldsymbol{\nabla}V_C(r)\;e^{i\chi_C(\mathbf{b})}, \tag{11}$$

where $\chi_C(\boldsymbol{b})$ is the Coulomb phase function,

$$\chi_C(\mathbf{b}) = \frac{-1}{v}\int_{-\infty}^{\infty} \mathrm{d}z\, V_C(\mathbf{b}, z)\ . \tag{12}$$

This expression for the amplitude is equally valid for extended nuclear-charge distributions provided the Coulomb potential is evaluated with the proper charge distribution [7].

We fist investigate the case of *point-like* nuclear charge. The Coulomb potential is then as in Eq.(10) and the corresponding Glauber expression for the Coulomb phase factor

$$e^{i\chi_C(b)} = \left(\frac{2a}{b}\right)^{i\eta} \tag{13}$$

where a is the cut-off radius in the Coulomb potential. For π^--nucleus scattering

$$\eta = 2Z\alpha/v. \tag{14}$$

The velocity v can in the following safely be put to unity. Thus, Eq.(9) recast to include Coulomb scattering becomes

$$\mathcal{M}_C = \frac{-Z\alpha}{2\pi i}\int \mathrm{d}^3 r e^{-i\mathbf{q}\cdot\mathbf{r}}\ \frac{\boldsymbol{g}\cdot\boldsymbol{r}}{r^3}\left(\frac{2a}{b}\right)^{i\eta}. \tag{15}$$

Integration over the z-variable yields a modified Bessel function. Integration over the angle of the vector $\boldsymbol{q}$ produces a factor $\boldsymbol{g}\cdot\boldsymbol{q}_\perp$. We extract this factor and introduce the notation $F_C(\boldsymbol{q})$ for the remaining factor, which is an off-shell-Coulomb-scattering amplitude. Hence,

$$\mathcal{M}_C = \boldsymbol{g}\cdot\boldsymbol{q}\ F_C(\boldsymbol{q}_\perp, q_\parallel) \tag{16}$$

The Coulomb-scattering amplitude is an integral over impact parameter

$$F_C(\boldsymbol{q}) = 2Z\alpha/q_\perp \int_0^\infty \mathrm{d}b J_1(q_\perp b)\{q_\parallel b K_1(q_\parallel b)\}\left(\frac{2a}{b}\right)^{i\eta}. \tag{17}$$

It is convenient to split off the point-Coulomb factor, writing

$$F_C(\boldsymbol{q}) = \frac{2Z\alpha(aq)^{i\eta}e^{i\sigma_\eta}}{\boldsymbol{q}^2}\ h_C(\boldsymbol{q}) \tag{18}$$

with η defined in Eq.(14) and

$$\sigma_\eta = 2\arg\Gamma(1 - i\eta/2). \tag{19}$$

The extracted phase factors in Eq.(18) are the same as in elastic Coulomb scattering, except that now

$$q = \sqrt{\boldsymbol{q}_\perp^2 + q_\parallel^2}. \tag{20}$$

Nucleus	z=1.0	z=0.5	z=0.0
C	1.0	0.998-i0.030	0.997-i0.044
Fe	1.0	0.963 -i0.125	0.943 -i0.179
Pb	1.0	0.717 -i 0.272	0.588-i0.352

TABLE I: Numerical values of the Coulomb form factor $h_C(z)$ with $z = q_\perp^2/(q_\perp^2 + q_\parallel^2)$.

In high-energy-elastic scattering the longitudinal-momentum transfer $q_\parallel$ vanishes. In that case q of Eq.(18) is interpreted as $q_\perp$.

The integration over impact parameter in Eq.(17) leads to a hypergeometric function. After some manipulations a simple result for the fom factor $h_C(\boldsymbol{q})$ emerges

$$h_C(\boldsymbol{q}) \;=\; \boldsymbol{q}^2/q_\perp(aq)^{-i\eta}e^{-i\sigma_\eta}\int_0^\infty \mathrm{d}bJ_1(q_\perp b)\{q_\parallel bK_1(q_\parallel b)\}\left(\frac{2a}{b}\right)^{i\eta}$$

$$=\; \Gamma(2-i\eta/2)\Gamma(1+i\eta/2)F(i\eta/2,1-i\eta/2;2;\frac{q_\perp^2}{q_\perp^2+q_\parallel^2}). \tag{21}$$

There are three values of the momentum transfer where the value of $h_C(\boldsymbol{q})$ is both simple and interesting;

$$h_C(q_\perp, q_\parallel = 0) \;=\; 1, \tag{22}$$

$$h_C(q_\perp = q_\parallel) \;=\; \frac{\Gamma(1-i\eta/2)\Gamma(1+i\eta/2)}{\Gamma(1+i\eta/4)\Gamma(\frac{1}{2}-i\eta/4)}\sqrt{\pi}, \tag{23}$$

$$h_C(q_\perp = 0, q_\parallel) \;=\; (1-i\eta/2)\frac{\pi\eta/2}{\sinh(\pi\eta/2)}; \tag{24}$$

corresponding to $z = 1$, $\frac{1}{2}$, and 0. The value in Eq.(22) applies to elastic scattering, and bremsstrahlung when the transverse momentum transfer is considerably larger that the longitudinal-minimum-momentum transfer. The value in Eq.(23) applies to bremsstrahlung at the peak where $q_\perp = q_\parallel$. The value in Eq.(24) applies to bremsstrahlung in the very forward direction where $q_\perp = 0$. In Table I we give numerical values for three nuclei. In the cross-section distribution it is $|h_C(z)|^2$ that enters.

The form factor $h_C(z)$, which could reduce the cross section at the Coulomb peak by as much as 50 %, has not always been included. The cross-section distributions in [4], e.g., are calculated in the Born approximation. In order to be valid in the very forward region of $q_\perp \approx q_\parallel$ those distributions should be multiplied by $|h_C(z)|^2$. The analysis of the Dubna experiment [6] was also done without explicitely mentioning this factor.

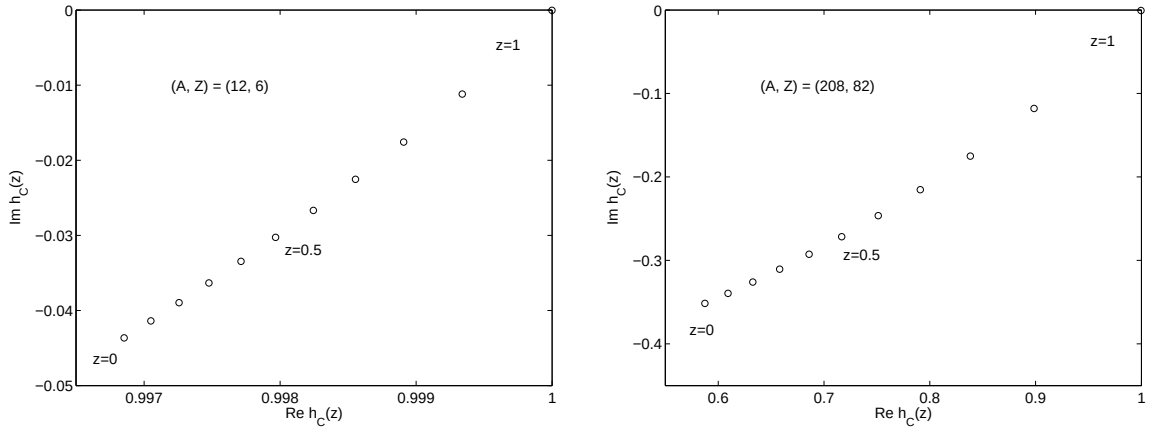

FIG. 1: Plots of the Coulomb-form factor $h_C(z)$ of Eq.(21) for carbon and lead. The circles mark points for values of z from 0 to 1.0, in steps of 0.1.

The above expressions for the Coulomb contribution to pionic bremsstrahlung are valid for point-like nuclear-charge distribution. The expression for the amplitude $\mathcal{M}_{\mathcal{C}}$ was given in Eq.(16) and for the form factor F_C in Eq.(17). This amplitude is summarized by the formula

$$\mathcal{M}_C = \boldsymbol{g} \cdot \boldsymbol{q}\ F_C(\boldsymbol{q}_\perp, q_\parallel). \tag{25}$$

The pion-nucleus-Coloumb-scattering amplitude differs slightly from the corresponding elastic amplitude since off-shell effects have been included through $q_\parallel$.

The finite extension of the nuclear-charge distribution can also be handled. We replace the point-Coulomb potential of Eq.(10) by the Coulomb potential $V_C^u(\boldsymbol{r})$, obtained from the extended-charge distribution. As a result Eq.(25) is replaced by

$$\mathcal{M}_C = \boldsymbol{g} \cdot \boldsymbol{q}\ F_C^u(\boldsymbol{q}_\perp, q_\parallel), \tag{26}$$

where $F_C^u(\boldsymbol{q}_\perp, q_\parallel)$ is the Coulomb-scattering amplitude of the extended-charge distribution.

The Coulomb-scattering amplitude for an extended-charge distridution cannot be calculated analytically. Therefore we divide the calculation into two steps, writing

$$F_C^u(\boldsymbol{q}_\perp, q_\parallel) \ = \ F_C^p(\boldsymbol{q}_\perp, q_\parallel) + \delta F_C^u(\boldsymbol{q}_\perp, q_\parallel) \tag{27}$$

$$\delta F_C^u(\boldsymbol{q}_\perp, q_\parallel) \ = \ F_C^u(\boldsymbol{q}_\perp, q_\parallel) - F_C^p(\boldsymbol{q}_\perp, q_\parallel), \tag{28}$$

where F_C^p is the point-like-form factor of Eq.(18). The advantage of this rearrangement is that $\delta F_C^u(\boldsymbol{q}_\perp, q_\parallel)$ is a smooth function of $q_\perp$ and $q_\parallel$ and easily calculated numerically, and

may in our bremsstrahlung application be evaluated at $q_\parallel = 0$.

From expression (11) for the bremsstrahlung amplitude we conclude that

$$\boldsymbol{g}\cdot\boldsymbol{q}\ \delta F_C(\boldsymbol{q}_\perp, q_\parallel) = \frac{-1}{2\pi i}\int \mathrm{d}^3 r e^{-i\mathbf{q}\cdot\mathbf{r}}\left[\boldsymbol{g}\cdot\boldsymbol{\nabla}V_C^u(r)e^{i\chi_C^u(\mathbf{b})} - \boldsymbol{g}\cdot\boldsymbol{\nabla}V_C(r)e^{i\chi_C(\mathbf{b})}\right], \tag{29}$$

where superscript u indicates potential and Coulomb phase of the the extended-charge distribution. We assume the nuclear charge to vanish outside a radius of R_u.

Rearrange the integrand as follows,

$$\begin{aligned}\boldsymbol{g}\cdot\boldsymbol{q}\ \delta F_C^u(\boldsymbol{q}_\perp, q_\parallel) \ =\ & \frac{-1}{2\pi i}\int \mathrm{d}^3 r e^{-i\mathbf{q}\cdot\mathbf{r}}\left[\boldsymbol{g}\cdot\boldsymbol{\nabla}(V_C^u(r) - V_C(r))e^{i\chi_C^u(\mathbf{b})}\right. \\ & \left. +\boldsymbol{g}\cdot\boldsymbol{\nabla}V_C(r)\ (e^{i\chi_C^u(\mathbf{b})} - e^{i\chi_C(\mathbf{b})})\right]. \end{aligned}\tag{30}$$

Then, the first term of the integrand vanishes for $r \geq R_u$, and since $R_u q_\parallel \ll 1$ we conclude that the dependence on $q_\parallel$ is so weak it can be ignored. In the second term we integrate over the z-variable and end up with a factor $bq_\parallel K_1(bq_\parallel)$. But the difference between the phase factors vanishes identically for $b \geq R_u$, so that everywhere $bq_\parallel \ll 1$. Again it is permissable to take the limit $q_\parallel \to 0$.

The result of this deliberation is that in Eq.(29) we can put $q_\parallel = 0$ and get

$$\delta F_C^u(\boldsymbol{q}_\perp, q_\parallel) \ =\ iv\int_0^{R_u} \mathrm{d}b\ b^2 \frac{J_1(bq_\perp)}{bq_\perp}\ \partial_b\left[e^{i\chi_C^u(\mathbf{b})} - e^{i\chi_C(\mathbf{b})}\right] \tag{31}$$

$$\ =\ -iv\int_0^{R_u} \mathrm{d}b\ bJ_0(q_\perp b)\left[e^{i\chi_C^u(b)} - e^{i\chi_C(b)}\right]. \tag{32}$$

The first version is the one best suited for numerical evaluation. The second version shows explicitely that δF_C^u is the difference between the Coulomb amplitudes for extended- and point-charge distributions.

In Fig. 2 we compare the three functions F_C^u, F_C^p, and δF_C^u. We have chosen $q_\parallel = 1.0$ MeV/c, a longitudinal-momentum transfer typical for the COMPASS experiment [3]. This number is so small that the position of the peak, at $q_\perp = q_\parallel$, cannot be seen in the figure where the curves plotted start at $q_\perp = 10$ MeV/c. As is evident, the point-like form factor is a good approximation to the uniform form factor up to about $q_\perp^2 = 0.001$ (GeV/c)^2.

We end this section by remarking that the Coulomb form factor discussed above is also encountered in ordinary Coulomb production

$$a + A \to a^\star + A,$$

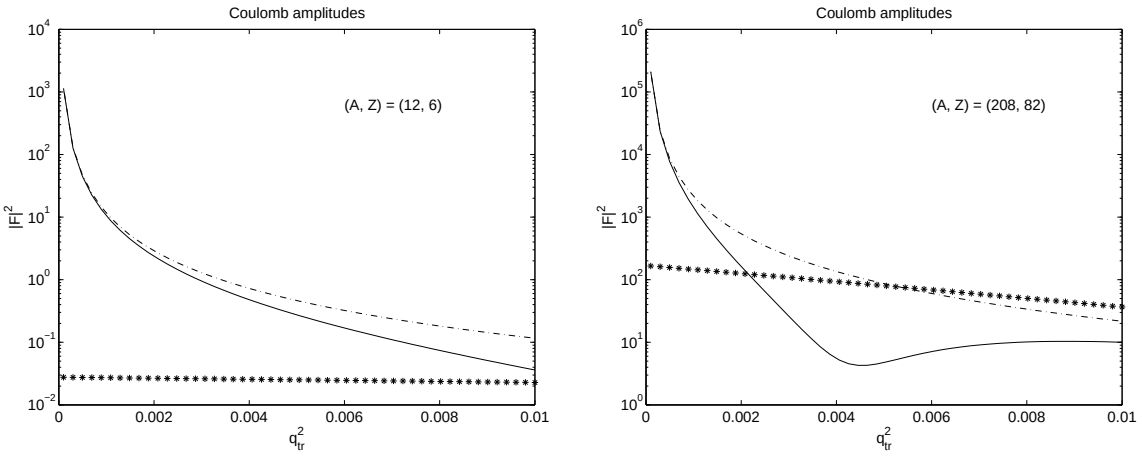

FIG. 2: Plots of the squared Coulomb form factors for $q_{\|} = 1.0$ MeV/c. The dashed curve corresponds the point-like form factor $F_C^p(\boldsymbol{q}_\perp, q_{\|})$ of Eq.(18), the starred curve to the difference form factor $\delta F_C^u(\boldsymbol{q}_\perp, q_{\|})$ of Eq.(32), and the solid line to their sum, the Coulomb form factor $F_C^u(\boldsymbol{q}_\perp, q_{\|})$ of Eq.(28). The unit for $\boldsymbol{q}_\perp^2$ is $(\mathrm{GeV}/c)^2$.

where the longitudinal-momentum transfer is defined as

$$q_{\|} = (m_{a^\star}^2 - m_a^2)/(2k), \tag{33}$$

with k the momentum of the incident particle a. In Refs [11, 12], and similar applications, the form factor is calculated numerically, but it is of course valuable to have an analytic expression for the point-like case. In many applications the dependence on $q_{\|}$ is very important, in contrast to the high-energy bremsstrahlung case discussed here.

III. THE NUCLEAR AMPLITUDE

It is important to have the correct phase between Coulomb and nuclear contributions. This point is treated in detail in Ref.[1]. Suppose the incident pion radiates a photon before scattering. Then the nuclear scattering is of course the compounded amplitude of Coulomb and nuclear scatterings. In Eq.(7) the contributions from radiation from external legs are summarized by the Born approximation to the pion structure functions, $A = 1$ and $B = 0$, changing $\boldsymbol{g}$ into $\boldsymbol{g}_0$ in Eq.(8). We want to extend this contribution by adding the nuclear scattering. To this end we simply replace the Coulomb potential $V_C(\boldsymbol{r})$ by the sum $V_C(\boldsymbol{r}) + V_N(\boldsymbol{r})$. As for the nuclear potential we assume the hadronic interaction between pion and nucleus to be the same for incident and emerging pions, even though their energies may be quite different. This is equivalent to saying that, within the Glauber model, we assume the pion-nucleon-cross section to be energy independent. This assumption can of course be relaxed.

The compounded nuclear and Coulomb amplitude correspondind to Eq.(9) thus reads

$$\mathcal{M}(\boldsymbol{q}) = \frac{-i}{2\pi} \int \mathrm{d}^3x \, e^{-i\mathbf{q}\cdot\mathbf{x}} \, \mathbf{g}_0 \cdot \nabla \left(V_C(\boldsymbol{r}) + V_N(\boldsymbol{r}) \right) e^{i(\chi_C(\mathbf{b}) + \chi_N(\mathbf{b}))}. \tag{34}$$

The momentum transfer $\mathbf{q}$ is three-dimensional and the distortion includes both Coulomb and hadronic distortion. The relation between potentials and phase-shift functions is defined in Eq.(12).

The integrand of Eq.(34) can be rearranged to read

$$\mathbf{g}_0 \cdot \nabla V_C(\boldsymbol{x}) e^{i\chi_C(\mathbf{b})} + \mathbf{g}_0 \cdot \nabla V_N(\boldsymbol{x}) e^{i(\chi_C(\mathbf{b}) + \chi_N(\mathbf{b}))} - \mathbf{g}_0 \cdot \nabla V_C(\boldsymbol{x}) e^{i\chi_C(\mathbf{b})} (1 - e^{i\chi_N(\mathbf{b})}). \tag{35}$$

The three terms are quite different in nature. The integrand of the first term extends over all of space, since the Coulomb potential does. The integrand of the second term is non-zero only inside the nucleus, since only there is the nuclear potential non-vanishing. Also the the integrand of the third term vanishes outside the nucleus, since the factor $(1 - e^{i\chi_N(\mathbf{b})})$ there does.

The first term of Eq.(35) describes the Coulomb contribution, for a general charge distribution. In the second and third terms we can neglect the functional dependence on the longitudinal momentum transfer, since $q_\parallel$ is fixed and so small that $R_u q_\parallel \ll 1$ for all nuclei. The nuclear contribution to the bremsstrahlung amplitude, i.e. the second and third terms

of Eq.(35), can be written as

$$\mathcal{M}_N(\boldsymbol{q}) \;=\; \mathbf{g}_0 \cdot \mathbf{q}\; F_N(\mathbf{q}_\perp), \tag{36}$$

$$F_N(\mathbf{q}_\perp) \;=\; \frac{iv}{2\pi}\int \mathrm{d}^2b\, e^{-i\mathbf{q}_\perp\cdot\mathbf{b}} e^{i\chi_C(\mathbf{b})}\left[1 - e^{i\chi_N(\mathbf{b})}\right]. \tag{37}$$

The factor $F_N(\mathbf{q}_\perp)$ is simply the elastic pion-nucleus scattering amplitude divided by the energy. It is energy independent since we assumed energy independent pion-nucleus interactions.

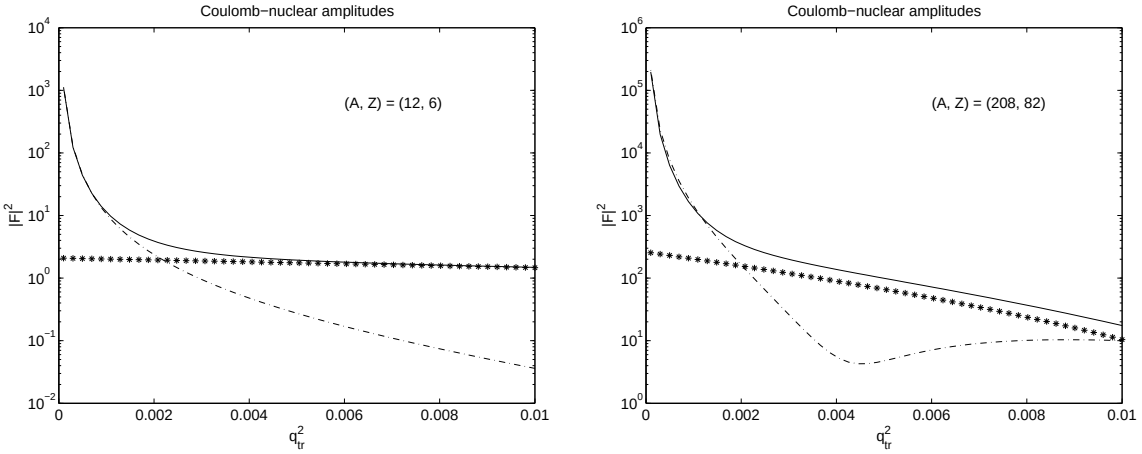

FIG. 3: Plots of the squared form factors. The dashed curve corresponds the uniform-Coulomb-form factor $F_C^u(\boldsymbol{q})$ of Eq.(28), the starred curve to the nuclear-form factor $F_N(\boldsymbol{q})$ of Eq.(37), and the solid line to their sum. The unit for $\boldsymbol{q}_\perp^2$ is $(\mathrm{GeV}/c)^2$.

In Fig. 3 we have plotted what essentially amounts to elastic pion-nucleus cross-section distributions. The dashed lines represent Coulomb scattering, the starred lines nuclear scattering, and the solid lines their sum. In all terms we have neglected the longitudinal-momentum transfer, being so incredibly small on the scale of momenta plotted. For transverse momentum transfers $q_\perp^2 \geq 0.002\ (\mathrm{GeV}/c)^2$ the hadronic contribution dominates the Coulomb contribution.

IV. THE POLARIZABILITY AMPLITUDE

Now, we have the complete amplitude for point-like pions. But the aim is to incorporate the pion polarizabilities, which are represented by the vector $\mathbf{g} - \mathbf{g}_0$ in the one-photon-exchange matrix element of Eq.(8). Including Coulomb and hadronic distortions gives, instead of Eq.(11), the polarizability amplitude

$$\mathcal{M}_P(\boldsymbol{q}) = \frac{-1}{2\pi i} \int \mathrm{d}^3 r e^{-i\mathbf{q}\cdot\mathbf{r}} (\boldsymbol{g} - \boldsymbol{g}_0) \cdot \boldsymbol{\nabla} V_C(r)\ e^{i(\chi_C(\mathbf{b}) + \chi_N(\mathbf{b}))}. \tag{38}$$

Following our welltrodden path we rewrite the distortion factor as

$$e^{i(\chi_C(\mathbf{b}) + \chi_N(\mathbf{b}))} = e^{i\chi_C(\mathbf{b})} - e^{i\chi_C(\mathbf{b})}(1 - e^{i\chi_N(\mathbf{b})}). \tag{39}$$

The first term in this decomposition yields upon integration the Coulomb scattering amplitude $F_C(\mathbf{q})$. The second term vanishes for impact parameters $b \geq R_u$, and leads to a smooth term, as discussed above, where we can take the limit $q_\parallel \to 0$. Our result for the polarizability contribution to the bremsstrahlung amplitude is therefore

$$\mathcal{M}_P(\boldsymbol{q}) \ = \ (\boldsymbol{g} - \boldsymbol{g}_0) \cdot \boldsymbol{q} F_P(\mathbf{q}), \tag{40}$$

$$F_P(\mathbf{q}) \ = \ F_C^u(\mathbf{q}) + \delta F_P(\mathbf{q}_\perp), \tag{41}$$

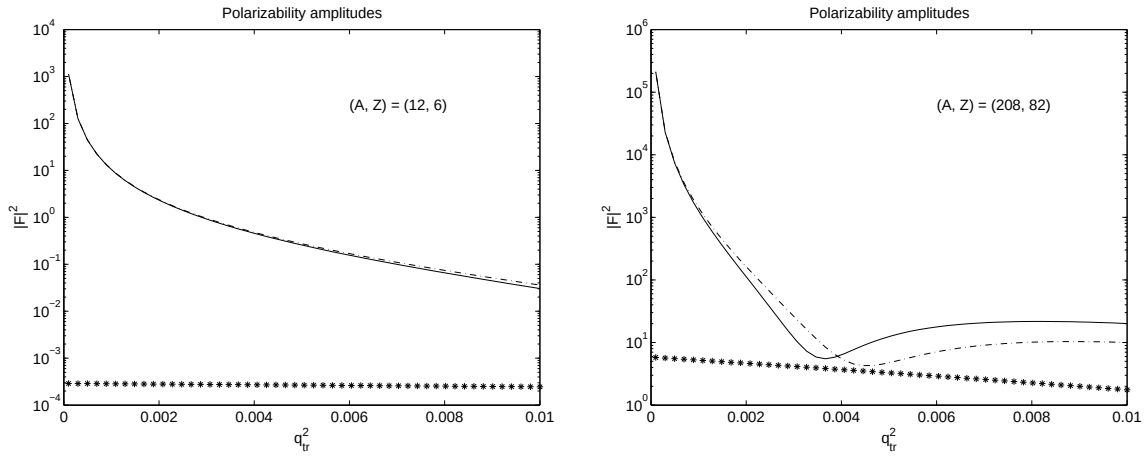

FIG. 4: Plots of the squared form factors. The dashed curve corresponds the uniform-Coulomb-form factor $F_C^u(\boldsymbol{q})$ of Eq.(28), the starred curve to the hadronic-distortion-form factor $\delta F_P(\boldsymbol{q}_\perp)$ of Eq.(42), and the solid line to their sum. The unit for $\boldsymbol{q}_\perp^2$ is $(\mathrm{GeV}/c)^2$.

with the hadronic contribution

$$\delta F_P(\mathbf{q}_\perp) = iv \int_0^{R_u} \mathrm{d}b\; b^2 \frac{J_1(bq_{1\perp})}{bq_{1\perp}} \left[\partial_b e^{i\chi_C^u(\mathbf{b})}\right] \left(1 - e^{i\chi_N(\mathbf{b})}\right). \tag{42}$$

This amplitude is a smooth function of $\mathbf{q}_\perp$. The fact that the hadronic distortion effects are quite different for the Born and the polarizability amplitudes was raised already in Ref.[1].

In Fig. 4 we graph the squared polarization-form factors. The dashed curve represents the Coulomb-scattering-form factor, the starred curve the hadronic-distortion-form factor, and the solid curve their sum. We see that hadronic effects are much weaker for the Compton polarizability amplitude than for the Compton Born amplitude, a conclusion that should be evident from expression (42), being proportional to the electromagnetic coupling as it is. Another conclusion that can be drawn from Fig. 4 is that the strength of the polarizability amplitude compared with that of the Born amplitude diminishes when the transverse momentum transfer moves into the region $q_\perp^2 \geq 0.002$ $(\mathrm{GeV}/c)^2$.

V. BREMSSTRAHLUNG CROSS-SECTION DISTRIBUTION

The complete pion-nucleus bremsstrahlung amplitude has a simple structure

$$\mathcal{M} = \boldsymbol{g}_0 \cdot \boldsymbol{q}_{1\perp}\ F_C(\boldsymbol{q}_1) + (\boldsymbol{g} - \boldsymbol{g}_0) \cdot \boldsymbol{q}_{1\perp}\ F_P(\boldsymbol{q}_1) + \boldsymbol{g}_0 \cdot \boldsymbol{q}_{1\perp}\ F_N(\boldsymbol{q}_{1\perp}), \tag{43}$$

where F_C is the off-shell pion-nucleus Coulomb scattering amplitude, F_N the on-shell pion-nucleus hadronic scattering amplitude, and F_P a mixed amplitude appropriate for the polarizability contribution. Moreover, F_P is essentially equal to F_C. The fact that the Coulomb amplitude is off-shell is only important in the region of the Coulomb peak, where $\boldsymbol{q}_{1\perp}$ is of a size similar to the constant $q_{1\parallel} = q_{min}$.

It is straightforward to calculate the cross-section distribution from Eq.(43). However, in practice the polarizability contributions are small, and in the expressions below it is often sufficient to keep the corresponding linear terms. After summation over the polarization directions of the final state photon we get for the cross-section distribution of Eq.(3)

$$\frac{\mathrm{d}\sigma}{\mathrm{d}^2 q_{1\perp} \mathrm{d}^2 q_{2\perp} \mathrm{d}x} = \frac{\alpha\ \mathbf{q}_{1\perp}^2}{\pi^2 m_\pi^4} \left(\frac{1-x}{x^3}\right) \left(\frac{x^2 m_\pi^2}{\mathbf{q}_{2\perp}^2 + x^2 m_\pi^2}\right)^2 \Big(\mathcal{K}_1 + \mathcal{K}_2 + \mathcal{K}_3\Big), \tag{44}$$

where $\mathcal{K}_1$ is the Coulomb-nuclear contribution for point-like pions

$$\mathcal{K}_1 \ = \ |F_C(\boldsymbol{q}_1) + F_N(\boldsymbol{q}_1)|^2 \left(1 - \mu^2 \frac{4x^2 m_\pi^2 \mathbf{q}_{2\perp}^2}{(x^2 m_\pi^2 + \mathbf{q}_{2\perp}^2)^2}\right), \tag{45}$$

$\mathcal{K}_2$ the contributions linear in the pion-polarizability functions

$$\begin{aligned} \mathcal{K}_2 \ = \ 2\Re\Big[\left(F_C^\star(\boldsymbol{q}_1) + F_N^\star(\boldsymbol{q}_1)\right) F_P(\boldsymbol{q}_1)\Big] \Big[C(x, \mathbf{q}_{2\perp}^2) \left(1 - \mu^2 \frac{4x^2 m_\pi^2 \mathbf{q}_{2\perp}^2}{(x^2 m_\pi^2 + \mathbf{q}_{2\perp}^2)^2}\right) \\ + B(x, \mathbf{q}_{2\perp}^2) \left(1 - \mu^2 \frac{2\mathbf{q}_{2\perp}^2}{x^2 m_\pi^2 + \mathbf{q}_{2\perp}^2}\right) \Big], \end{aligned} \tag{46}$$

and finally, $\mathcal{K}_3$ the contributions quadratic in the pion-polarizability functions

$$\mathcal{K}_3 \ = \ |F_P(\boldsymbol{q}_1)|^2 \Big[\Big|C(x, \mathbf{q}_{2\perp}^2)\Big|^2 \left(1 - \mu^2 \frac{4x^2 m_\pi^2 \mathbf{q}_{2\perp}^2}{(x^2 m_\pi^2 + \mathbf{q}_{2\perp}^2)^2}\right) + \Big|B(x, \mathbf{q}_{2\perp}^2)\Big|^2 \tag{47}$$

$$+ 2\Re\left(C(x, \mathbf{q}_{2\perp}^2) B^\star(x, \mathbf{q}_{2\perp}^2)\right) \left(1 - \mu^2 \frac{2\mathbf{q}_{2\perp}^2}{x^2 m_\pi^2 + \mathbf{q}_{2\perp}^2}\right) \Big], \tag{48}$$

where, in order to shorten the expressions, we have introduced

$$A(x, \mathbf{q}_{2\perp}^2) = 1 + C(x, \mathbf{q}_{2\perp}^2). \tag{49}$$

The parameter μ is defined as $\mu = \hat{\mathbf{q}}_{1\perp} \cdot \hat{\mathbf{q}}_{2\perp}$. On the right hand sides of the above formulae we may in most applications replace μ^2 by its average $\frac{1}{2}$.

The dominant contribution to the cross section Eq.(44) comes from the point-like-pion approximation, i.e. the contribution proportional to $\mathcal{K}_1$ of Eq.(45). The polarizbility contributions are contained in $\mathcal{K}_2$ and $\mathcal{K}_3$. Experiments are aimed at measuring the contribution proportional to $\mathcal{K}_2$, which is linear in the polarizabilities. The relative nuclear-form factor between the $\mathcal{K}_2$ and $\mathcal{K}_1$ contributions is

$$R(\boldsymbol{q}_1) = \frac{F_P(\boldsymbol{q}_1)}{F_C(\boldsymbol{q}_1) + F_N(\boldsymbol{q}_1)}, \tag{50}$$

with the polarizability-form factor $F_P(\boldsymbol{q}_1)$ as defined in Eq.(41), and with $\boldsymbol{q}_1$ the momentum transfer to the nucleus. When hadronic interactions of the pions are neglected, the ratio $R(\boldsymbol{q}_1)$ becomes one. In Fig. 5 we plot this ratio as a function of $\boldsymbol{q}_{1\perp}^2$ in the interval $0 \leq \boldsymbol{q}_{1\perp}^2 \leq 0.002$ (GeV/c)^2.

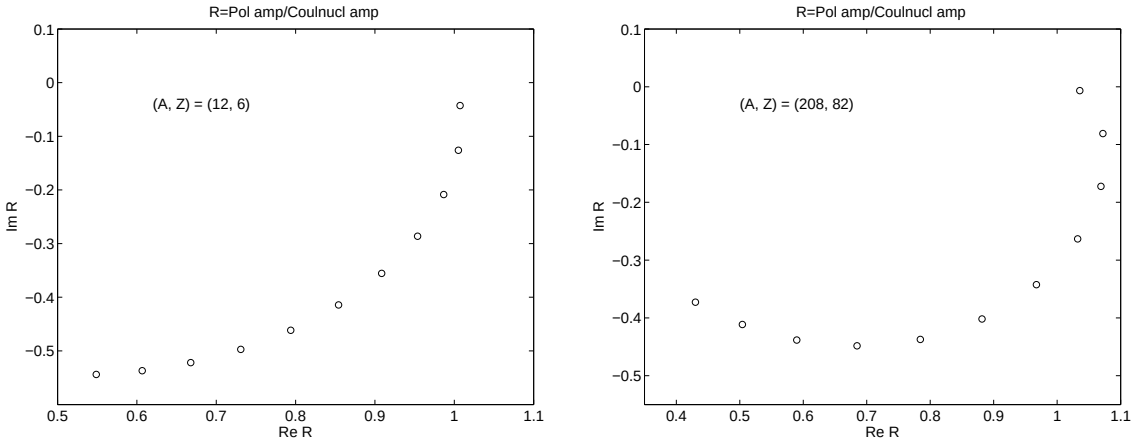

FIG. 5: Plots of the ratio $R(\boldsymbol{q}_1)$ of the form factors for the linear polarizability cross-section contribution and the point-like-pion cross-section contribution, of Eq.(50). The circles represent the ratios for $\boldsymbol{q}_{1\perp}^2$ in the interval $0 \leq \boldsymbol{q}_{1\perp}^2 \leq 0.002$ (GeV/c)^2 in steps of 0.0002 (GeV/c)^2. The value of $R(\boldsymbol{q}_1)$ is one at $\boldsymbol{q}_{1\perp}^2 = 0$. The unit for $\boldsymbol{q}_\perp^2$ is (GeV/c)^2.

In Fig. 5 we have limited the region of $\boldsymbol{q}_{1\perp}^2$, since we know from the graphs of the previous sections that for $\boldsymbol{q}_{1\perp}^2 \geq 0.002$ (GeV/c)^2 the contributions from the hadronic interactions of the pions play a dominant role. Of course, our model is valid also in this case, but experimenters prefer to stay in the region where the description is simple, meaning $R(\boldsymbol{q}_1) = 1$. From Fig. 5 we conclude that if this is desired we must further restrict the momentum transfer to the nucleus. For Compton masses in the threshold region, sufficiently below

the ρ-meson mass, the polarizability functions $C(x, \mathbf{q}_{2\perp}^2)$ and $B(x, \mathbf{q}_{2\perp}^2)$ of Eq.(46) are real-valued functions. Therefore, in the threshold region only the real part of $R(\boldsymbol{q}_1)$ matters and limiting ourselves to $\boldsymbol{q}_{1\perp}^2 \leq 0.001$ (GeV/c)^2, it is reasonable to set $R(\boldsymbol{q}_1) \approx 1$. In the general case, however, the more detailed model developed here must be applied.

VI. SUMMARY

The pion-Compton scattering amplitude is near threshold fixed by Born terms involving pion-exchange diagrams (Thompson scattering). At higher energies structure dependent terms enter, labeled electric and magnetic polarizabilities (Rayleigh scattering). Those terms can be modelled as σ-, ρ-, and a_1-exchange contributions.

Pion-nucleus bremsstrahlung is closely related to pion-Compton scattering. At small momentum transfers to the nucleus the bremsstrahlung reaction is dominated by single-photon exchange between the pion and the nucleus. As a consequence, the bremsstrahlung amplitude becomes propotional to the pion-Compton scattering amplitude, the initial photon of the Compton scattering being the virtual photon the pion is exchanging with the nucleus.

For heavy nuclei multiple-photon exchange becomes important. But its sole effect is to introduce the well-known Coulomb phase factor. In the bremsstrahlung reaction the phase is slightly different from the one in elastic Coulomb scattering, since in bremsstrahlung there is a fixed longitudinal momentum transfer to the nucleus, q_{min}. A second effect produced by the longitudinal momentum transfer is the appearance of a new form factor. An analytic form for this form factor is given, for the first time. It is important for heavy nuclei when the transverse momentum transfer to the nucleus is similar in magnitude to q_{min}.

However, pionic bremsstrahlung can also be accompanied by pion-nucleus hadronic scattering. The importance of this contribution increases as the transverse momentum transfer increases, exactly as in elastic scattering. It affects both Born and polarizability parts of the Compton amplitudes. The Born term becomes, essentially, multiplied by the sum of elastic Coulomb and hadronic pion-nucleus scattering amplitudes. For the polarizability terms there is a corresponding sum, but whereas the Coulomb amplitude is the same, the hadronic one is different and substantially weaker.

Numerical estimates of the various contributions are presented. The outcome is that if one is interested in extracting polarizability contributions, it is advantageous to restrict oneself to momentum transfers $q_\perp^2 \leq 0.001$ $(\mathrm{GeV}/c)^2$, since there the ratio between polarizability and Born contributions remains essentially the same as in free pion Compton scattering. Increasing the momentum transfer means increasing the importance of hadronic scattering. The ratio then changes in an important way, and varies with momentum transfer. Pushing into the momentum transfers region $q_\perp^2 \geq 0.002$ $(\mathrm{GeV}/c)^2$ we come into a region where

hadronic scattering dominates, and where in addition the contribution from the polarizability terms diminishes.

VII. APPENDIX

In this Appendix we explain how we have calculated the Coulomb and nuclear amplitudes. It is then important to remember that we need the amplitudes only for small momentum transfers, meaning that the structure of the nuclear surface region will not be important. Hence, we choose uniform nuclear charge and matter distributions and with the same radii, $R_u = 1.1A^{1/3}$ fm. More sophisticated calculations are straightforward but also more time consuming.

We start with the *Coulomb amplitude*. The Coulomb phase contains a cut-off a that should go to infinity. In this limit the cut-off enters as a phase factor common to both Coulomb and nuclear amplitudes. The value of a is therefore immaterial and we may simply replace $2a$ by R_u. We also put $v = 1$.

The Coulomb-phase function for a uniform-charge distribution is

$$\chi_C^u(b) \;=\; 2Z\alpha\ln(R_u/b), \qquad b > R_u$$

$$\;=\; 2Z\alpha\left[\left(\frac{1}{3}+\frac{2b^2}{3R_u^2}\right)\sqrt{1-b^2/R_u^2}-\ln\left(1+\sqrt{1-b^2/R_u^2}\right)\right], \qquad b < R_u. \quad (51)$$

We shall also need the derivatives

$$b\partial_b\chi_C^u(b) \;=\; -2Z\alpha, \qquad b > R_u$$

$$\;=\; 2Z\alpha\left(\frac{b}{R_u}\right)^2\left[2\sqrt{1-b^2/R_u^2}-\frac{1}{1+\sqrt{1-b^2/R_u^2}}\right], \qquad b < R_u. \quad (52)$$

The Coulomb-phase function for a point-charge distribution is

$$\chi_C(b) = 2Z\alpha\ln(R_u/b). \quad (53)$$

The Coulomb-scattering amplitude $F_C^u(\boldsymbol{q}_1)$ is decomposed as in Eq.(27). It is written as a sum of two terms; the point-Coulomb amplitude and a correction term, $\delta F_C^u(\boldsymbol{q}_1)$. The point amplitude is calculated exactly. The correction term is the difference between the Coulomb amplitudes for exteneded and point charges, respectively. In this term the fixed longitudinal momentum transfer can be put to zero. The difference is calculated numerically from the formula

$$\delta F_C^u(\boldsymbol{q}_{1\perp}, q_{1\parallel}) = i\int_0^{R_u}\mathrm{d}b\; b^2\frac{J_1(q_{1\perp}b)}{q_{1\perp}b}\;\partial_b\left[e^{i\chi_C^u(b)}-e^{i\chi_C(b)}\right]. \quad (54)$$

The integral in the last step extends over the nuclear charge distribution alone.

Next we look at the *nuclear amplitude* of Eq.(37).

$$F_N(q_\perp) = i\int_0^\infty \mathrm{d}b\; bJ_0(q_\perp b)e^{i\chi_C^u(b)}\left[1 - e^{i\chi_N(b)}\right]. \tag{55}$$

The nuclear phase-shift function is related to the target-thickness function $T_A(b)$ by

$$i\chi_N(b) = -\tfrac{1}{2}\sigma(1 - i\alpha)T_A(b), \tag{56}$$

where σ is the pion-nucleon total cross section, and α the ratio of real to imaginary part of the forward elastic pion-nucleon scattering amplitude. The target-thickness function for a nucleus of uniform density is

$$T_A(b) = \frac{3A}{2\pi R_u^2}\sqrt{1 - b^2/R_u^2}. \tag{57}$$

We have chosen numerical values for the hadronic parameters appropriate for pions of 190 GeV/c; i.e. $\sigma = 24.1$ mb and $\alpha = -0.06$ [13, 14].

[1] G. Fäldt, Phys. Rev. C **76**, 014608 (2007).

[2] G. Fäldt and U. Tengblad, Phys. Rev. C **76**, 064607 (2007).

[3] J. Friedrich, Hadron07, Frascati, 2007 (unpublished).

[4] G. Fäldt and U. Tengblad, Phys. Rev. C **xx**, xxxx (2008).

[5] A. S. Gal'perin et al., Sov. J. Nucl. Phys. **32**, 545 (1980).

[6] Yu. M. Antipov et al., Phys. Lett. B **121**, 445 (1983); Yu. M. Antipov et al., Z. Phys. C **24**, 39 (1984); Yu. M. Antipov et al., Z. Phys. C **26**, 495 (1985).

[7] R.J. Glauber, in *Lectures in theoretical physics*, edited by W.E. Brittin and L.G. Dunham (Interscience, New York, 1959), vol. 1, p. 315; in *High-Energy physics and Nuclear Structure*, edited by S. Devons (Plenum, New York, 1970), p. 207.

[8] J. F. Donoghue and B. R. Holstein, Phys. Rev. D **48**, 37 (1993).

[9] J. Ahrens et al., Eur. Phys. J. A **23**, 113 (2005).

[10] G. Fäldt and I. Hulthage, Nucl. Phys. A **302**, 433 (1978).

[11] G. Fäldt et al., Nucl. Phys. B **41**, 124 (1972).

[12] C. Bemporad et al., Nucl. Phys. B **51**, 1 (1973).

[13] A. S. Carroll et al., Phys. Lett. B **80**, 423 (1979).

[14] J. P. Burq et al., Phys. Lett. B **109**, 111 (1982).